Article

Sequential Electron-Transfer and Proton-Transfer Pathways in Hydride-Transfer Reactions from Dihydronicotinamide Adenine Dinucleotide Analogues to Non-heme Oxoiron(IV) Complexes and *p*-Chloranil. Detection of Radical Cations of NADH Analogues in Acid-Promoted Hydride-Transfer Reactions

Shunichi Fukuzumi, Hiroaki Kotani, Yong-Min Lee, and Wonwoo Nam

J. Am. Chem. Soc., **2008**, 130 (45), 15134-15142 • DOI: 10.1021/ja804969k • Publication Date (Web): 21 October 2008

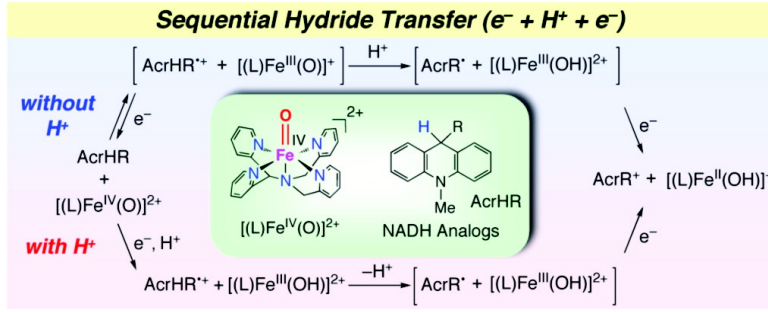

More About This Article

Additional resources and features associated with this article are available within the HTML version:

- Supporting Information
- Access to high resolution figures
- Links to articles and content related to this article
- Copyright permission to reproduce figures and/or text from this article

View the Full Text HTML

J|A|C|S
ARTICLES

Published on Web 10/21/2008

Sequential Electron-Transfer and Proton-Transfer Pathways in Hydride-Transfer Reactions from Dihydronicotinamide Adenine Dinucleotide Analogues to Non-heme Oxoiron(IV) Complexes and *p*-Chloranil. Detection of Radical Cations of NADH Analogues in Acid-Promoted Hydride-Transfer Reactions

Shunichi Fukuzumi,*,† Hiroaki Kotani,† Yong-Min Lee,‡ and Wonwoo Nam*,‡

Department of Material and Life Science, Graduate School of Engineering, Osaka University, SORST, Japan Science and Technology Agency (JST), Suita, Osaka 565-0871, Japan, and Department of Chemistry and Nano Science, Center for Biomimetic Systems, Ewha Womans University, Seoul 120-750, Korea

Received June 28, 2008; E-mail: fukuzumi@chem.eng.osaka-u.ac.jp; wwnam@ewha.ac.kr

Abstract: Hydride transfer from dihydronicotinamide adenine dinucleotide (NADH) analogues, such as 10-methyl-9,10-dihydroacridine ($AcrH_2$) and its derivatives, 1-benzyl-1,4-dihydronicotinamide (BNAH), and their deuterated compounds, to non-heme oxoiron(IV) complexes such as $[(L)Fe^{IV}(O)]^{2+}$ (L = N4Py, Bn-TPEN, and TMC) occurs to yield the corresponding NAD^+ analogues and non-heme iron(II) complexes in acetonitrile. Hydride transfer from the NADH analogues to *p*-chloranil (Cl_4Q) also occurs to produce the corresponding NAD^+ analogues and the hydroquinone anion (Cl_4QH^-). The logarithms of the observed second-order rate constants (log k_H) of hydride transfer from NADH analogues to non-heme oxoiron(IV) complexes are linearly correlated with those of hydride transfer from the same series of NADH analogues to Cl_4Q, including similar kinetic deuterium isotope effects. The log k_H values of hydride transfer from NADH analogues to non-heme oxoiron(IV) complexes are also linearly correlated with those of deprotonation of the radical cations of NADH analogues. Such linear correlations indicate that overall hydride-transfer reactions of NADH analogues to both non-heme oxoiron(IV) complexes and Cl_4Q occur via electron transfer from NADH analogues to the oxoiron(IV) complexes, followed by rate-limiting deprotonation from the radical cations of NADH analogues and subsequent rapid electron transfer from the deprotonated radicals to the Fe(III) complexes to yield the corresponding NAD^+ analogues and the Fe(II) complexes. The electron-transfer pathway was accelerated by the presence of perchloric acid, and the resulting radical cations of NADH analogues were detected by electron spin resonance spectroscopy and UV−vis spectrophotometry in the acid-promoted hydride-transfer reactions from NADH analogues to non-heme oxoiron(IV) complexes. This result provides the first direct evidence that a hydride transfer from NADH analogues to non-heme oxoiron(IV) complexes proceeds via an electron-transfer pathway.

Introduction

Non-heme iron enzymes are involved in metabolically important oxidative transformations, in which high-valent oxoiron(IV) species are frequently invoked as the key intermediates responsible for the oxidation of organic substrates.[1] Within the past five years, non-heme oxoiron(IV) intermediates have been characterized in the catalytic cycles of *Escherichia coli* taurine: α-ketogultarate dioxygenase (TauD), prolyl-4-hydroxylase, and halogenase CytC3.[2] These results demonstrate unambiguously that non-heme oxoiron(IV) intermediates are capable of abstracting C−H bonds of substrates in biological reactions. In biomimetic studies, a non-heme oxoiron(IV) intermediate was characterized spectroscopically by Wieghardt and co-workers for the first time.[3] Subsequently, the first crystal structure of an oxoiron(IV) complex, $[(TMC)Fe^{IV}(O)]^{2+}$ (TMC = 1,4,8,11-tetramethyl-1,4,8,11-tetraazacyclotetradecane), was obtained in the reaction of $[Fe^{II}(TMC)]^{2+}$ and artificial oxidants.[4] Since then, extensive efforts have been devoted to examining the reactivities of mononuclear non-heme oxoiron(IV) complexes bearing tetradentate N4 and pentadentate N5 and N4S ligands in the

† Osaka University.
‡ Ewha Womans University.

(1) (a) Kryatov, S. V.; Rybak-Akimova, E. V.; Schindler, S. *Chem. Rev.* **2005**, *105*, 2175–2226. (b) Abu-Omar, M. M.; Loaiza, A.; Hontzeas, N. *Chem. Rev.* **2005**, *105*, 2227–2252. (c) Borovik, A. S. *Acc. Chem. Res.* **2005**, *38*, 54–61. (d) Costas, M.; Mehn, M. P.; Jensen, M. P.; Que, L., Jr. *Chem. Rev.* **2004**, *104*, 939–986.

(2) (a) Krebs, C.; Galonić Fujimori, D. G.; Walsh, C. T.; Bollinger, J. M., Jr. *Acc. Chem. Res.* **2007**, *40*, 484–492. (b) Price, J. C.; Barr, E. W.; Tirupati, B.; Bollinger, J. M., Jr.; Krebs, C. *Biochemistry* **2003**, *42*, 7497–7508. (c) Price, J. C.; Barr, E. W.; Glass, T. E.; Krebs, C.; Bollinger, J. M., Jr. *J. Am. Chem. Soc.* **2003**, *125*, 13008–13009. (d) Riggs-Gelasco, P. J.; Price, J. C.; Guyer, R. B.; Brehm, J. H.; Barr, E. W.; Bollinger, J. M., Jr.; Krebs, C. *J. Am. Chem. Soc.* **2004**, *126*, 8108–8109. (e) Hoffart, L. M.; Barr, E. W.; Guyer, R. B.; Bollinger, J. M., Jr.; Krebs, C. *Proc. Natl. Acad. Sci. U.S.A.* **2006**, *103*, 14738–14743. (f) Galonić, D. P.; Barr, E. W.; Walsh, C. T.; Bollinger, J. M., Jr.; Krebs, C. *Nat. Chem. Biol.* **2007**, *3*, 113–116.

(3) Grapperhaus, C. A.; Mienert, B.; Bill, E.; Weyhermüller, T.; Wieghardt, K. *Inorg. Chem.* **2000**, *39*, 5306–5317.

 10.1021/ja804969k CCC: $40.75

oxidation of various substrates, including alkane hydroxylation, olefin epoxidation, alcohol oxidation, *N*-dealkylation, and the oxidation of sulfides and PPh_3.[5−8] More recently, we have reported the electron-transfer properties (i.e., the reorganization energies and the one-electron reduction potentials) of non-heme oxoiron(IV) complexes.[9] However, hydride-transfer reactions of non-heme oxoiron(IV) complexes have never been explored previously.[10]

Among hydride donors, dihydronicotinamide adenine dinucleotide (NADH) and analogues have attracted particular interest, because NADH is the most important source of hydride ion (two electrons and a proton) in biological redox reactions.[11−13] There has been extensive discussion on the mechanism of hydride-transfer reactions of NADH and analogues, such as concerted hydride transfer vs sequential electron−proton−electron (equivalent to a hydride ion) transfer.[14−24] In contrast to the one-step hydride-transfer pathway that proceeds without an intermediate, the electron-transfer pathway would produce radical cations of NADH and its analogues as reaction intermediates.[25,26] Such an electron-transfer pathway can be accelerated by an acid due to the protonation of the one-electron-reduced species.[27−31] Indeed, we have recently reported the successful detection of a radical cation of an NADH analogue, 9,10-dihydro-10-methylacridine ($AcrH_2$), in the acid-promoted hydride transfer from $AcrH_2$ to 1-(*p*-tolylsulfinyl)-2,5-benzoquinone.[32] However, the hydride-transfer mechanism has yet to be clarified in the case of non-heme oxoiron(IV) complexes. Also, *neither* the effect of acid on hydride-transfer reactions from NADH analogues to non-heme oxoiron(IV) complexes *nor* the detection of radical cations of NADH analogues in the hydride-transfer reactions has so far been reported.

We report herein the first example of hydride transfer from a series of NADH analogues, 10-methyl-9,10-dihydroacridine ($AcrH_2$) and its 9-subsituted derivatives (AcrHR: R = H, Ph, Me, and Et), 1-benzyl-1,4-dihydronicotinamide (BNAH), and their deuterated compounds, to mononuclear non-heme oxoiron(IV) complexes, $[(L)Fe^{IV}(O)]^{2+}$ (L = N4Py, *N*,*N*-bis(2-pyridylmethyl)-*N*-bis(2-pyridyl)methylamine; Bn-TPEN, *N*-benzyl-*N*,*N*′,*N*′-tris(2-pyridylmethyl)ethane-1,2-diamine; TMC, 1,4,8,11-tetramethyl-1,4,8,11-tetraazacyclotetradecane) (see Chart 1). The mechanism of hydride transfer from NADH analogues to non-heme oxoiron(IV) complexes is clarified in relation to hydride transfer from the same series of NADH analogues to a *p*-benzoquinone derivative.[22] The promoting effect of perchloric acid on hydride-transfer reactions from NADH analogues to $[(L)Fe^{IV}(O)]^{2+}$ is extensively compared with the hydride-transfer reactions without acids. In addition, we have succeeded in detecting radical cations of NADH analogues in acid-promoted hydride-transfer reactions from NADH analogues to $[(L)Fe^{IV}(O)]^{2+}$. This result provides direct evidence that hydride transfer

(4) Rohde, J.-U.; In, J.-H.; Lim, M. H.; Brennessel, W. W.; Bukowski, M. R.; Stubna, A.; Münck, E.; Nam, W.; Que, L., Jr. *Science* **2003**, *299*, 1037–1039.

(5) (a) Nam, W. *Acc. Chem. Res.* **2007**, *40*, 522–531. (b) Que, L., Jr. *Acc. Chem. Res.* **2007**, *40*, 493–500.

(6) (a) Kaizer, J.; Klinker, E. J.; Oh, N. Y.; Rohde, J.-U.; Song, W. J.; Stubna, A.; Kim, J.; Münck, E.; Nam, W.; Que, L., Jr. *J. Am. Chem. Soc.* **2004**, *126*, 472–473. (b) Oh, N. Y.; Suh, Y.; Park, M. J.; Seo, M. S.; Kim, J.; Nam, W. *Angew. Chem., Int. Ed.* **2005**, *44*, 4235–4239. (c) Kim, S. O.; Sastri, C. V.; Seo, M. S.; Kim, J.; Nam, W. *J. Am. Chem. Soc.* **2005**, *127*, 4178–4179. (d) Bukowski, M. R.; Koehntop, K. D.; Stubna, A.; Bominaar, E. L.; Halfen, J. A.; Münck, E.; Nam, W.; Que, L., Jr. *Science* **2005**, *310*, 1000–1002. (e) Park, M. J.; Lee, J.; Suh, Y.; Kim, J.; Nam, W. *J. Am. Chem. Soc.* **2006**, *128*, 2630–2634. (f) Sastri, C. V.; Oh, K.; Lee, Y. J.; Seo, M. S.; Shin, W.; Nam, W. *Angew. Chem., Int. Ed.* **2006**, *45*, 3992–3995. (g) Nehru, K.; Seo, M. S.; Kim, J.; Nam, W. *Inorg. Chem.* **2007**, *46*, 293–298. (h) Sastri, C. V.; Lee, J.; Oh, K.; Lee, Y. J.; Lee, J.; Jackson, T. A.; Ray, K.; Hirao, H.; Shin, W.; Halfen, J. A.; Kim, J.; Que, L., Jr.; Shaik, S.; Nam, W. *Proc. Natl. Acad. Sci. U.S.A.* **2007**, *104*, 19181–19186.

(7) (a) Martinho, M.; Banse, F.; Bartoli, J.-F.; Mattioli, T. A.; Battioni, P.; Horner, O.; Bourcier, S.; Girerd, J.-J. *Inorg. Chem.* **2005**, *44*, 9592–9596. (b) Balland, V.; Charlot, M.-F.; Banse, F.; Girerd, J.-J.; Mattioli, T. A.; Bill, E.; Bartoli, J.-F.; Battioni, P.; Mansuy, D. *Eur. J. Inorg. Chem.* **2004**, *n/a*, 301–308.

(8) (a) Bautz, J.; Comba, P.; Lopez de Laorden, C. L.; Menzel, M.; Rajaraman, G. *Angew. Chem., Int. Ed.* **2007**, *46*, 8067–8070. (b) Anastasi, A. E.; Comba, P.; McGrady, J.; Lienke, A.; Rohwer, H. *Inorg. Chem.* **2007**, *46*, 6420–6426. (c) Bautz, J.; Bukowski, M. R.; Kerscher, M.; Stubna, A.; Comba, P.; Lienke, A.; Münck, E.; Que, L., Jr. *Angew. Chem., Int. Ed.* **2006**, *45*, 5681–5684.

(9) Lee, Y.-M.; Kotani, H.; Suenobu, T.; Nam, W.; Fukuzumi, S. *J. Am. Chem. Soc.* **2008**, *130*, 434–435.

(10) Electron-transfer, hydride-transfer, and hydrogen−atom transfer mechanisms have been discussed in hydrocarbon oxidation by bis-μ-oxo manganese dimers: Larsen, A. S.; Wang, K.; Lockwood, M. A.; Rice, G. L.; Won, T.-J.; Lovell, S.; Sadı´lek, M.; Tureček, F.; Mayer, J. M. *J. Am. Chem. Soc.* **2002**, *124*, 10112–10123.

(11) Stout, D. M.; Meyers, A. I. *Chem. Rev.* **1982**, *82*, 223–243.

(12) Gebicki, J.; Marcinek, A.; Zielonka, J. *Acc. Chem. Res.* **2004**, *37*, 379–386.

(13) (a) Fukuzumi, S. In *Advances in Electron Transfer Chemistry*; Mariano, P. S., Ed.; JAI press; Greenwich, CT, 1992; pp 67−175. (b) Fukuzumi, S.; Tanaka, T. In *Photoinduced Electron Transfer*; Fox, M. A., Chanon, M., Eds.; Elsevier: Amsterdam, 1988; Part C, Chap. 10, pp 578−635.

(14) (a) He, G.-X.; Blasko, A.; Bruice, T. C. *Bioorg. Chem.* **1993**, *21*, 423–430. (b) Ohno, A. *J. Phys. Org. Chem.* **1995**, *8*, 567–576.

(15) Fukuzumi, S.; Koumitsu, S.; Hironaka, K.; Tanaka, T. *J. Am. Chem. Soc.* **1987**, *109*, 305–316.

(16) (a) Fukuzumi, S.; Nishizawa, N.; Tanaka, T. *J. Org. Chem.* **1984**, *49*, 3571–3578. (b) Fukuzumi, S.; Nishizawa, N.; Tanaka, T. *J. Chem. Soc., Perkin Trans. 2* **1985**, *49*, 371–378.

(17) (a) Pestovsky, O.; Bakac, A.; Espenson, J. H. *J. Am. Chem. Soc.* **1998**, *120*, 13422–13428. (b) Pestovsky, O.; Bakac, A.; Espenson, J. H. *Inorg. Chem.* **1998**, *37*, 1616–1622.

(18) (a) Zhu, X.-Q.; Yang, Y.; Zhang, M.; Cheng, J.-P. *J. Am. Chem. Soc.* **2003**, *125*, 15298–15299. (b) Zhu, X.-Q.; Cao, L.; Liu, Y.; Yang, Y.; Lu, J.-Y.; Wang, J.-S.; Cheng, J.-P. *Chem.-Eur. J.* **2003**, *9*, 3937–3945. (c) Zhu, X.-Q.; Zhang, J.-Y.; Cheng, J.-P. *J. Org. Chem.* **2006**, *71*, 7007–7015.

(19) Afanasyeva, M. S.; Taraban, M. B.; Purtov, P. A.; Leshina, T. V.; Grissom, C. B. *J. Am. Chem. Soc.* **2006**, *128*, 8651–8658.

(20) Yuasa, J.; Yamada, S.; Fukuzumi, S. *J. Am. Chem. Soc.* **2006**, *128*, 14938–14948.

(21) (a) Fukuzumi, S.; Ohkubo, K.; Okamoto, T. *J. Am. Chem. Soc.* **2002**, *124*, 14147–14155. (b) Fukuzumi, S.; Fujii, Y.; Suenobu, T. *J. Am. Chem. Soc.* **2001**, *123*, 10191–10199. (c) Fukuzumi, S.; Yuasa, J.; Suenobu, T. *J. Am. Chem. Soc.* **2002**, *124*, 12566–12573.

(22) Fukuzumi, S.; Ohkubo, K.; Tokuda, Y.; Suenobu, T. *J. Am. Chem. Soc.* **2000**, *122*, 4286–4294.

(23) Lee, I.-S. H.; Jeoung, E. H.; Kreevoy, M. M. *J. Am. Chem. Soc.* **1997**, *119*, 2722–2728.

(24) (a) Carlson, B. W.; Miller, L. L. *J. Am. Chem. Soc.* **1985**, *107*, 479–485. (b) Miller, L. L.; Valentine, J. R. *J. Am. Chem. Soc.* **1988**, *110*, 3982–3989.

(25) Fukuzumi, S.; Tokuda, Y.; Kitano, T.; Okamoto, T.; Otera, J. *J. Am. Chem. Soc.* **1993**, *115*, 8960–8968.

(26) (a) Fukuzumi, S.; Inada, O.; Suenobu, T. *J. Am. Chem. Soc.* **2002**, *124*, 14538–14539. (b) Fukuzumi, S.; Inada, O.; Suenobu, T. *J. Am. Chem. Soc.* **2003**, *125*, 4808–4816.

(27) (a) Fukuzumi, S. In *Electron Transfer in Chemistry*; Balzani, V., Ed.; Wiley-VCH: Weinheim, 2001; Vol. 4, pp 3−67. (b) Fukuzumi, S. *Org. Biomol. Chem.* **2003**, *1*, 609–620.

(28) (a) Fukuzumi, S.; Ishikawa, M.; Tanaka, T. *J. Chem. Soc., Perkin Trans. 2* **1989**, 1037–1045. (b) Fukuzumi, S.; Mochizuki, S.; Tanaka, T. *J. Am. Chem. Soc.* **1989**, *111*, 1497–1499.

(29) Fukuzumi, S.; Tokuda, Y. *J. Phys. Chem.* **1993**, *97*, 3737–3741.

(30) (a) Coleman, C. A.; Rose, J. G.; Murray, C. J. *J. Am. Chem. Soc.* **1992**, *114*, 9755–9762. (b) Murray, C. J.; Webb, T. *J. Am. Chem. Soc.* **1991**, *113*, 7426–7427.

(31) Yuasa, J.; Yamada, S.; Fukuzumi, S. *J. Am. Chem. Soc.* **2008**, *130*, 5808–5820.

(32) Yuasa, J.; Yamada, S.; Fukuzumi, S. *Angew. Chem., Int. Ed.* **2008**, *47*, 1068–1071.

Chart 1

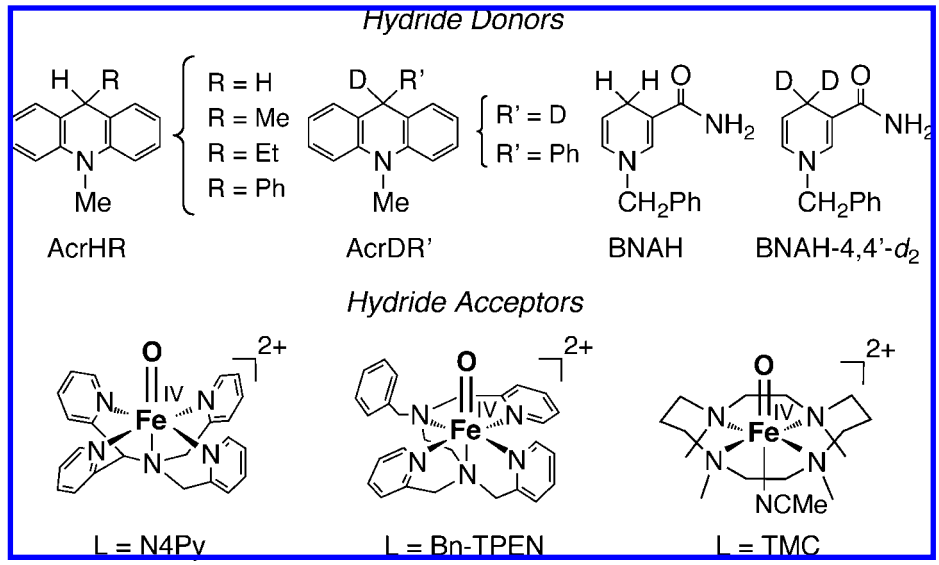

from NADH analogues to non-heme oxoiron(IV) complexes proceeds via an electron-transfer pathway.

Experimental Section

Materials. Commercially available reagents, 1-benzyl-1,4-dihydronicotinamide (BNAH), 9-phenyl-10-methylacridinium ion (Acr^+-Ph), 10-methylacridone, acridine, methyl iodide (MeI), $NaBH_4$, *p*-chloranil (Cl_4Q), and ferrocene from Tokyo Chemical Industry Co., Ltd., and $LiAlD_4$ and $NaBD_4$ from CIL, Inc., were of the best available purity and used without further purification unless otherwise noted. Acetonitrile (MeCN) and ether were dried according to the literature procedures and distilled under Ar prior to use.[33] Iodosylbenzene (PhIO) was prepared by a literature method.[4,6e] Non-heme iron(II) complexes, $Fe(TMC)(CF_3SO_3)_2$, $Fe(N4Py)(CF_3SO_3)_2$, and $Fe(Bn\text{-}TPEN)(CF_3SO_3)_2$, and their oxoiron(IV) complexes, $[(TMC)Fe^{IV}(O)]^{2+}$, $[(N4Py)Fe^{IV}(O)]^{2+}$, and $[(Bn\text{-}TPEN)Fe^{IV}(O)]^{2+}$, were prepared by the literature methods.[4,6a]For example, $[(TMC)Fe^{IV}(O)]^{2+}$ was prepared by reacting $Fe(TMC)(CF_3SO_3)_2$ (0.5 mM) with 1.2 equiv of PhIO (0.6 mM) in CH_3CN at ambient temperature. 10-Methyl-9,10-dihydroacridine ($AcrH_2$) was prepared from 10-methylacridinium iodide ($AcrH^+I^-$) by reduction with $NaBH_4$ in methanol and purified by recrystallization from ethanol.[25] $AcrH^+I^-$ was prepared by the reaction of acridine with MeI in acetone, converted to the perchlorate salt ($AcrH^+ClO_4^-$) by the addition of magnesium perchlorate to $AcrH^+I^-$, and purified by recrystallization from methanol.[25] The dideuterated compound, [9,9′-$^2H_2$]-10-methylacridine ($AcrD_2$), was prepared from 10-methylacridone by reduction with $LiAlD_4$ in ether.[25] 9-Substituted (9-alkyl or 9-phenyl) 10-methyl-9,10-dihydroacridine (AcrHR; R = Me, Et, and Ph) was prepared by the reduction of $AcrH^+I^-$ with the corresponding Grignard reagents (RMgX).[25] AcrDPh was prepared by reducing Acr^+-Ph with $NaBD_4$ and purified by recrystallization from ethanol. 9-Substituted 10-methylacridinium perchlorate ($AcrR^+ClO_4^-$; R = Me, Et, and Ph) was prepared by the reaction of 10-methylacridone in dichloromethane with the corresponding Grignard reagents (RMgX) and purified by recrystallization from ethanol−diethyl ether.[22] The dideuterated compound, 1-benzyl-1,4-dihydro[4,4′-$^2H_2$]nicotinamide (BNAH-4,4′-d_2), was prepared from monodeuterated compound (BNAH-4-d_1)[34] by three cycles of oxidation with *p*-chloranil in dimethylformamide and reduction with dithionite in deuterium oxide.[35]

Caution: *Perchlorate salts are potentially explosive and should be handled with care!*

Reaction Procedure. Typically, $AcrH_2$ (1.0×10^{-3} M) was added to a CD_3CN solution (0.6 mL) containing $[(N4Py)Fe^{IV}(O)]^{2+}$ (1.0×10^{-3} M) in an NMR tube. The reaction was complete in 10 min under these conditions. The products were identified as $AcrH^+$ and $[(N4Py)Fe^{II}]^{2+}$ by comparing their ^1H NMR spectra with those in the literature.[36] ^1H NMR measurements were performed with a JMN-AL-300 (300 MHz) NMR spectrometer at 298 K. ^1H NMR (CD_3CN): $AcrH^+$, δ 4.75 (s, 3H), 7.98 (t, 2H), 8.41 (t, 2H), 8.50 (d, 2H), 8.54 (d, 2H), 9.86 (s, 1H); $[(N4Py)Fe^{II}]^{2+}$, δ 4.25−4.45 (m, 4H), 6.32 (s, 1H), 7.04 (d, 2H), 7.35 (m, 4H), 7.69 (m, 2H), 7.80−7.90 (m, 4H), 8.92 (d, 2H), 9.01 (d, 2H).

Spectral Measurements. Hydride transfer from $AcrH_2$ to $[(N4Py)Fe^{IV}(O)]^{2+}$ (5.0×10^{-5} M) was examined by monitoring spectral changes in the presence of appropriate amounts of $AcrH_2$ (1.0×10^{-3}−5.0×10^{-3} M) at 298 K with a Hewlett-Packard 8453 photodiode-array spectrophotometer and a quartz cuvette (path length = 10 mm). Typically, a deaerated MeCN solution of $[(N4Py)Fe^{IV}(O)]^{2+}$ (5.0×10^{-5} M) was added with a microsyringe to a deaerated MeCN solution containing $AcrH_2$.

Kinetic Measurements. Kinetic measurements were performed on a UNISOKU RSP-601 stopped-flow spectrometer equipped with a MOS-type highly sensitive photodiode-array or a Hewlett-Packard 8453 photodiode-array spectrophotometer at 298 K. Rates of hydride transfer from AcrHR derivatives to $[(L)Fe^{IV}(O)]^{2+}$ (L = N4Py, Bn-TPEN, and TMC) were monitored by the increase and decrease of absorption bands due to Acr^+-R ($\lambda_{max} = 358$ nm, $\epsilon_{max} = 1.80 \times 10^4$ M^{-1} cm^{-1})[22] and $[(L)Fe^{IV}(O)]^{2+}$ (L = N4Py, $\lambda_{max} = 695$ nm; Bn-TPEN, $\lambda_{max} = 739$ nm; and TMC, $\lambda_{max} = 820$ nm). Rates of hydride transfer from AcrHR to Cl_4Q were determined from the appearance of the absorbance due to $AcrR^+$ or the radical anion ($Cl_4Q^{\bullet-}$: $\lambda_{max} =$ 585 nm, $\epsilon_{max} = 5.6 \times 10^3$ M^{-1} cm^{-1}).[22] The concentration of AcrHR or BNAH was maintained at more than 10-fold excess of the other reactant to attain pseudo-first-order conditions. Pseudo-first-order rate constants were determined by a least-squares curve fit. The first-order plots were linear for three or more half-lives, with the correlation coefficient $\rho > 0.999$. In each case, it was confirmed that the rate

(33) Armarego, W. L. F.; Chai, C. L. L. *Purification of Laboratory Chemicals*, 5th ed.; Butterworth Heinemann: Amsterdam, 2003.

(34) (a) Anderson, A. G., Jr.; Berkelhammer, G. *J. Am. Chem. Soc.* **1958**, *80*, 992–999. (b) Mauzerall, D.; Westheimer, F. H. *J. Am. Chem. Soc.* **1955**, *77*, 2261–2264.

(35) Caughey, W.; Schellenberg, K. A. *J. Org. Chem.* **1966**, *31*, 1978–1982.

(36) (a) Fukuzumi, S.; Okamoto, K.; Tokuda, Y.; Gros, C. P.; Guilard, R. *J. Am. Chem. Soc.* **2004**, *126*, 17059–17066. (b) Lubben, M.; Meetsma, A.; Wilkinson, E. C.; Feringa, B.; Que, L., Jr. *Angew. Chem., Int. Ed. Engl.* **1995**, *34*, 1512–1514.

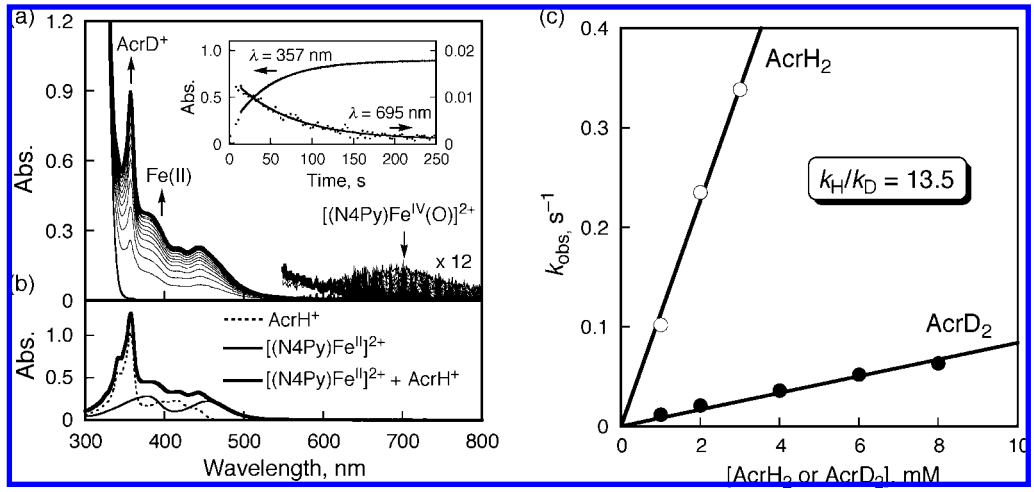

Figure 1. (a) Spectral changes observed in the reaction of $[(N4Py)Fe^{IV}(O)]^{2+}$ (5.0×10^{-5} M) and $AcrD_2$ (2.0×10^{-3} M) in deaerated MeCN at 298 K. Inset: Time profiles of absorption changes at $\lambda = 357$ and 695 nm for the formation of $AcrH^+$ and decay of $[(N4Py)Fe^{IV}(O)]^{2+}$, respectively. (b) UV−vis spectra of $AcrH^+$ (6.0×10^{-5} M) and $[(N4Py)Fe^{II}]^{2+}$ (6.0×10^{-5} M) in MeCN. (c) Plots of the pseudo-first-order rate constants (k_{obs}) of $[(N4Py)Fe^{IV}(O)]^{2+}$ vs $AcrH_2$ (○) or $AcrD_2$ (●).

constants derived from at least five independent measurements agreed within an experimental error of ±5%.

Electron Spin Resonance (ESR) Measurement. ESR detection of $AcrDPh^{\bullet+}$ was performed as follows. Typically, a MeCN solution of $[(N4Py)Fe^{IV}(O)]^{2+}$ (1.0×10^{-4} M) in the presence of $HClO_4$ (1.0×10^{-3} M) in an ESR cell (3.0 mm i.d.) was purged with nitrogen for 5 min. AcrDPh (1.0×10^{-2} M) was then added to the solution, which was already cooled near the melting point of MeCN. The mixed solution was immediately cooled to 77 K in a liquid N_2 dewar for ESR measurements. The ESR spectrum of $AcrDPh^{\bullet+}$ was recorded on a JEOL JES-RE1XE spectrometer at 77 K in frozen MeCN. The magnitude of modulation was chosen to optimize the resolution and signal-to-noise (S/N) ratio of the observed spectra under nonsaturating microwave power conditions. The g value was calibrated using an Mn^{2+} marker ($g = 2.034$, 1.981). Computer simulation of the ESR spectra was carried out by using Calleo ESR version 1.2 (Calleo Scientific Publisher) on a personal computer.

Results and Discussion

Hydride Transfer from NADH Analogues to Non-heme Oxoiron(IV) Complexes. The visible spectral changes in hydride transfer from an NADH analogue ($AcrH_2$) to $[(N4Py)Fe^{IV}(O)]^{2+}$ are shown in Figure 1a, where the absorption band at 695 nm due to $[(N4Py)Fe^{IV}(O)]^{2+}$ decreases, accompanied by an increase in the absorption band at 357 nm due to 10-methylacridinium ion ($AcrH^+$) and the absorption bands at 380 and 450 nm due to $[(N4Py)Fe^{II}]^{2+}$. The spectrum after the reaction, as shown in Figure 1a, agrees well with the superposition of the $AcrH^+$ and $[(N4Py)Fe^{II}]^{2+}$ spectra (Figure 1b). Thus, the stoichiometry of the reaction is given by eq 1.[37]

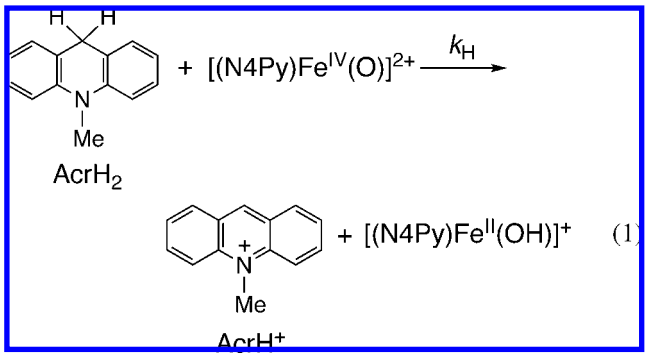

The formation rate of $AcrH^+$, which was determined from an increase in absorbance at 357 nm, coincides with the decay rate of $[(N4Py)Fe^{IV}(O)]^{2+}$ determined from a decrease in absorbance at 695 nm (Figure 1a, inset). The rates obey pseudo-first-order kinetics in the presence of a large excess of $AcrH_2$, and the pseudo-first-order rate constants (k_{obs}) increase linearly with the increase of the $AcrH_2$ concentration (Figure 1c, ○). The second-order rate constant (k_H) for the reaction of $[(N4Py)Fe^{IV}(O)]^{2+}$ and $AcrH_2$ was determined to be 1.1×10^2 M^{-1} s^{-1} from the linear plot of k_{obs} vs concentration of $AcrH_2$. When $AcrH_2$ was replaced by the dideuterated compound ($AcrD_2$), a large deuterium kinetic isotope effect (KIE) value of 13.5 was observed (Figure 1c, ●).

The rate of hydride transfer from 1-benzyl-1,4-dihydronicotinamide (BNAH) to $[(N4Py)Fe^{IV}(O)]^{2+}$, which was much faster than the reaction rate of $AcrH_2$, was determined using a stopped-flow technique. The formation of $[(N4Py)Fe^{II}]^{2+}$ is seen as a recovery of bleaching absorption at 450 nm in the difference transient absorption spectrum, and this is accompanied by the decay of the absorbance at 695 nm due to $[(N4Py)Fe^{IV}(O)]^{2+}$, as shown in Figure 2a. Both the formation and decay rates obey pseudo-first-order kinetics with the same slopes (Figure 2a, inset). The k_H values of BNAH and the dideuterated compound (BNAH-4,4′-d_2) were determined to be 7.8×10^2 and 1.7×10^2 M^{-1} s^{-1}, respectively, giving a KIE value of 4.6 (Figure 2b). Hydride-transfer reactions were also investigated with other NADH analogues and non-heme oxoiron(IV) complexes, and the k_H values for other NADH analogues are listed in Table 1 (see the columns k_H ($[(L)Fe^{IV}(O)]^{2+}$)).

Hydride Transfer from NADH Analogues to *p*-Chloranil. It has been reported previously that hydride-transfer reactions from $AcrH_2$ and BNAH to hydride acceptors such as

(37) $[(L)Fe^{III}(OH)]^{2+}$ was not detected in the course of the reaction owing to the rapid electron transfer from the resulting $AcrH^{\bullet}$ to $[(L)Fe^{III}(OH)]^{2+}$. $[(L)Fe^{II}]^{2+}$ was produced from $[(L)Fe^{II}(OH)]^+$ by protonation and dehydration due to residual water contained in MeCN. The formation of $AcrH^+$ and $[(N4Py)Fe^{II}]^{2+}$ was also confirmed by ^1H NMR (see Experimental Section).

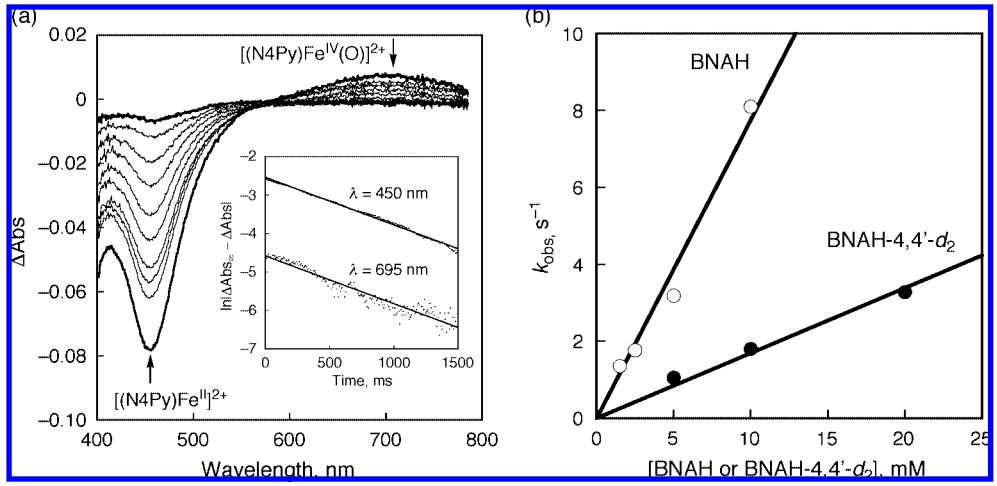

Figure 2. (a) UV−vis spectral changes observed in hydride transfer from BNAH-4,4′-d_2 (5.0×10^{-3} M) to $[(N4Py)Fe^{IV}(O)]^{2+}$ (3.0×10^{-5} M) in MeCN at 298 K. Inset: First-order plots at $\lambda = 450$ and 695 nm. (b) Plots for the determination of second-order rate constants (k_H) in the reactions of $[(N4Py)Fe^{IV}(O)]^{2+}$ with [BNAH (○) or BNAH-4,4′-d_2 (●)].

Table 1. Oxidation Potentials (E_{ox}) of NADH Analogues, Rate Constants (k_d) of Deprotonation of Radical Cations of NADH Analogues, and Rate Constants (k_H) for the Reactions of Hydride Transfer from NADH Analogues to Cl_4Q and Oxoiron(IV) Complexes ($[(L)Fe^{IV}(O)]^{2+}$) in Deaerated MeCN at 298 K

					k_H ($[(L)Fe^{IV}(O)]^{2+}$), M^{-1} s^{-1}		
	NADH analogue	E_{ox}[a] (V vs SCE)	k_d,[b] s^{-1}	k_H (Cl_4Q), M^{-1} s^{-1}	L = N4Py	L = Bn-TPEN	L= TMC
1	BNAH	0.57	2.4×10	1.0×10^3	7.8×10^2	1.8×10^4	
2	BNAH-4,4′-d_2	0.57	1.8×10	1.9×10^2	1.7×10^2	2.2×10^3	
3	$AcrH_2$	0.81	6.4	1.5×10	1.1×10^2	1.3×10^3	4.0×10^2
4	$AcrD_2$	0.81	7.1×10^{-1}	1.7	8.4	7.4×10	7.0×10
5	AcrHMe	0.84	1.1	9.4×10^{-1}	1.0×10	6.2×10	
6	AcrHPh	0.88	4.1	6.6×10^{-1}	1.1×10	7.0×10	
7	AcrHEt	0.84	4.9×10^{-1}	4.6×10^{-1}	4.0	2.0×10	
8	AcrDPh	0.88	n.d.	1.3×10^{-1}	8.0×10^{-1}	4.0	

[a] Taken from ref 22. [b] Taken from ref 25.

p-chloranil (eq 2)[15] and tetracyanoethylene (TCNE)[38] occur efficiently, followed by a subsequent fast electron transfer

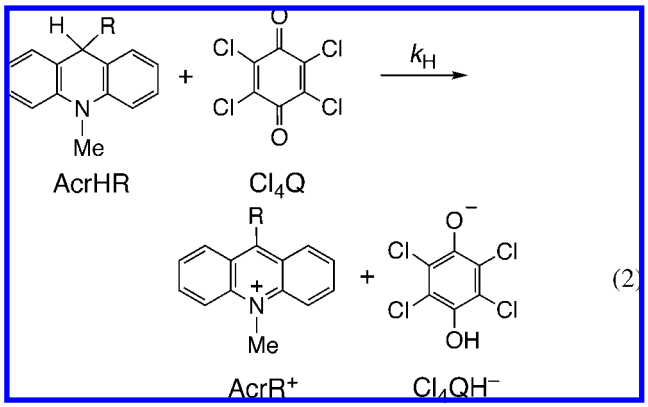

(2)

from the reduced product (Cl_4QH^-) to the hydride acceptors and disproportionation of the resulting radical. We have also reported previously that hydride transfer from a series of AcrHR to hydride acceptors such as 2,3-dichloro-5,6-dicyano-*p*-benzoquinone (DDQ) proceeds via sequential electron and proton transfer, followed by rapid electron transfer, rather than one-step hydride transfer.[22] In order to compare the hydride-transfer reactivity between non-heme oxoiron(IV) complexes and a *p*-benzoquinone derivative, we determined the rate constants of hydride-transfer reactions from the same series of NADH analogues to *p*-chloranil (Cl_4Q) as employed in the reactions of non-heme oxoiron(IV) complexes. The k_H values determined are listed in Table 1 (see the column k_H (Cl_4Q)).

Comparison of the Hydride-Transfer Reactivity of Non-heme Oxoiron(IV) Complexes vs *p*-Chloranil. It should be noted that the k_H value for hydride transfer from BNAH to Cl_4Q (1.0×10^3 M^{-1} s^{-1}) is similar to the k_H value for hydride transfer from BNAH to $[(N4Py)Fe^{IV}(O)]^{2+}$ (7.8×10^2 M^{-1} s^{-1}). This result indicates that the reactivity of $[(N4Py)Fe^{IV}(O)]^{2+}$ is similar to that of Cl_4Q in hydride-transfer reactions. Similar reactivity between non-heme oxoiron(IV) complexes and Cl_4Q is further exemplified in Figure 3, which shows a comparison of the k_H values between $[(L)Fe^{IV}(O)]^{2+}$ and Cl_4Q for hydride-transfer reactions of NADH analogues. The k_H values determined in the reactions of $[(L)Fe^{IV}(O)]^{2+}$ and Cl_4Q vary significantly depending on NADH analogues, in particular on the substituent R in AcrHR. The significant decrease in the reactivity upon the introduction of a substituent R at the C-9 position can hardly be reconciled by a one-step hydride-transfer mechanism. The alkyl or phenyl group at the C-9 position is known to be in a boat axial conformation, and thereby the hydrogen at the C-9 position is located at the equatorial position, where steric hindrance due to the axial substituent is minimized in the hydride-transfer reactions.[25] The introduction of an electron-donating substituent R would activate the release of a

(38) Fukuzumi, S.; Kondo, Y.; Tanaka, T. *J. Chem. Soc., Perkin Trans. 2* **1984**, 673–679.

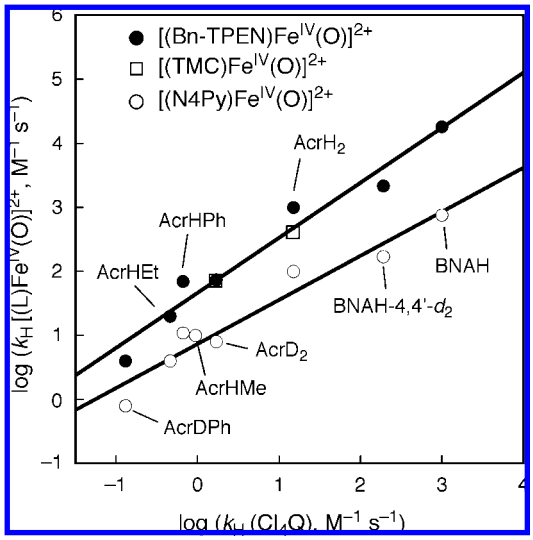

Figure 3. Plots of k_H for hydride transfer from NADH analogues to [(Bn-TPEN)Fe^{IV}(O)]$^{2+}$ (●), [(TMC)Fe^{IV}(O)]$^{2+}$ (□), and [(N4Py)Fe^{IV}(O)]$^{2+}$ (○) vs k_H for hydride transfer from the same series of NADH analogues to Cl_4Q in MeCN at 298 K.

negatively charged hydride ion if the concerted hydride transfer should take place. The remarkable decrease in the reactivity with the increasing electron-donor ability of R rather indicates that the reactivity is determined by the process in which a positive charge is released. Further, there is an excellent linear correlation between the k_H values of hydride-transfer reactions of NADH analogues with [(L)Fe^{IV}(O)]$^{2+}$ and the corresponding values with Cl_4Q.

Mechanism of Hydride Transfer from NADH Analogues to Non-heme Oxoiron(IV) Complexes. Linear correlations between hydride-transfer reactions of NADH analogues with [(L)Fe^{IV}(O)]$^{2+}$ and Cl_4Q in Figure 3 imply that the hydride-transfer mechanism of [(L)Fe^{IV}(O)]$^{2+}$ is virtually the same as that of Cl_4Q. Although there is still debate on the mechanism(s) of hydride transfer from NADH analogues to hydride acceptors in terms of an electron-transfer pathway vs a one-step hydride-transfer pathway, the electron-transfer pathway is now well accepted for hydride transfer from NADH analogues to hydride acceptors that are strong electron acceptors.[13−24] It should be noted that the E_{red} values of non-heme oxoiron(IV) complexes ([(L)Fe^{IV}(O)]$^{2+}$: 0.39−0.51 V vs SCE)[9] are more positive than that of Cl_4Q (0.01 V vs SCE).[15] This means that the [(L)Fe^{IV}(O)]$^{2+}$ complexes are much stronger electron acceptors than Cl_4Q. Thus, the electron transfer from NADH analogues (AcrHR) to [(L)Fe^{IV}(O)]$^{2+}$ is highly likely to occur, and this is followed by rapid proton transfer from AcrHR$^{\bullet+}$ to [(L)Fe^{III}(O)]$^{+}$ and electron transfer from the resulting AcrR$^{\bullet}$ to [(L)Fe^{III}(OH)]$^{2+}$, affording the final products, AcrH^{+} and [(L)Fe^{II}(OH)]$^{+}$, as shown in Scheme 1.

We have previously succeeded in detecting transient absorption and ESR spectra of AcrHR$^{\bullet+}$ and BNAH$^{\bullet+}$ produced by the electron-transfer oxidation of AcrHR and BNAH by [Fe(phen)$_3$]$^{3+}$ (phen = 1,10-phenanthroline), respectively.[25,26] The transient absorption spectra of AcrHR$^{\bullet+}$ exhibit diagnostic long-wavelength absorption maxima at λ_{max} = 640−710 nm, depending on the substituent R.[25] The decay of AcrHR$^{\bullet+}$ obeyed first-order kinetics, and the decay rate constant of AcrHR$^{\bullet+}$ (k_d) corresponds to the rate constant of deprotonation from AcrHR$^{\bullet+}$ to produce AcrR$^{\bullet}$.[25] The k_d value becomes smaller by changing R from H to Ph, Me, and Et (see the column k_d in Table 1).[25] The introduction of a substituent R at the C-9 position in $AcrH_2$ causes an increase in the magnitude of nonplanarity of the acridine ring, as indicated by the decrease in the hyperfine coupling constant of the C-9 equatorial proton in AcrHR$^{\bullet+}$, resulting in an increase in the deprotonation barrier to form the planar AcrR$^{\bullet}$.[25,39,40] Since the E_{ox} values of AcrHR are rather invariant irrespective of the difference in R,[25] the variation in the reactivity of AcrHR in the hydride-transfer reactions by [(L)Fe^{IV}(O)]$^{2+}$ in Figure 3 may result from the difference in the reactivity of the proton-transfer step from AcrHR$^{\bullet+}$ to [(L)Fe^{III}(O)]$^{+}$ following the initial electron transfer. Thus, the k_H values of hydride transfer from NADH analogues to [(L)Fe^{IV}(O)]$^{2+}$ obtained in the present study are linearly correlated well with the rate constants of deprotonation of NADH radical cations (k_d), as shown in Figure 4.[25,26]

The initial electron-transfer step from NADH analogues (e.g., AcrHR) to [(L)Fe^{IV}(O)]$^{2+}$ (k_{et}) is endergonic ($\Delta G_{et} > 0$), judging from the E_{ox} values of AcrHR (e.g., 0.81 V vs SCE for $AcrH_2$)[15] and E_{red} values of [(L)Fe^{IV}(O)]$^{2+}$ (e.g., 0.51 V vs SCE for [(N4Py)Fe^{IV}(O)]$^{2+}$).[9] The subsequent proton-transfer step from AcrHR$^{\bullet+}$ to [(L)Fe^{III}(O)]$^{+}$ (k_p) competes with the back-electron-transfer step (k_{-et}). The final electron-transfer step from AcrR$^{\bullet}$ to [(L)Fe^{III}(OH)]$^{2+}$ must occur rapidly because this step is highly exergonic ($\Delta G_{et} \ll 0$) based on the negative E_{ox} values of AcrR$^{\bullet}$ (e.g., −0.46 V vs SCE for AcrH$^{\bullet}$)[25] and positive E_{red} values of [(L)Fe^{III}(OH)]$^{2+}$ (vide supra).[9] In such a case, the observed rate constant (k_H) is given by eq 3.

$$k_H = k_p k_{et}/(k_{-et} + k_p) \quad (3)$$

When $k_p \gg k_{-et}$, k_H corresponds to k_{et}, and the rate-determining step is the initial electron-transfer step, which would exhibit no deuterium KIE. The observation of significant deuterium KIEs (Figures 1c and 2b) indicates that $k_p \ll k_{-et}$ when k_H corresponds to $k_p(k_{et}/k_{-et})$. Thus, the observed deuterium KIEs are ascribed to the proton-transfer step from the radical cations of NADH analogues to [(L)Fe^{III}(O)]$^{+}$. The k_H/k_D value of 4.6 for hydride transfer from BNAH to [(N4Py)Fe^{IV}(O)]$^{2+}$ is similar to the k_H/k_D value of 5.3 for the hydride transfer from BNAH to Cl_4Q. In the case of $AcrH_2$, however, the k_H/k_D value of 13.5 for [(N4Py)Fe^{IV}(O)]$^{2+}$ is larger than the value of 8.8 for Cl_4Q. The latter big discrepancy is ascribed to the fact that k_H/k_D values vary depending on the pK_a values of radical cations of NADH analogues, $Cl_4QH^{\bullet}$ and [(L)Fe^{III}(OH)]$^{2+}$.

Detection of Radical Cations of NADH Analogues in Acid-Promoted Hydride Transfer from NADH Analogues to Non-heme Oxoiron(IV) Complexes. The electron-transfer pathway of hydride transfer from AcrHR to [(L)Fe^{IV}(O)]$^{2+}$ was confirmed by the direct detection of the radical cation (AcrHR$^{\bullet+}$) that is produced in the acid-promoted hydride transfer from AcrHR to [(L)Fe^{IV}(O)]$^{2+}$ (vide infra). We have previously reported that hydride transfer from $AcrH_2$ to a *p*-benzoquinone derivative, 1-(*p*-tolylsulfinyl)-2,5-benzoquinone (TolSQ), is made possible by the presence of perchloric acid ($HClO_4$) (eq 4).[32] The promoting effect of $HClO_4$ on hydride transfer from

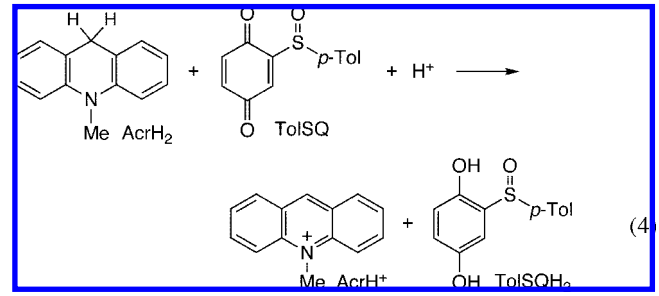

(4)

Scheme 1. Proposed Mechanism of the Hydride Transfer from AcrHR to $[(L)Fe^{IV}(O)]^{2+}$

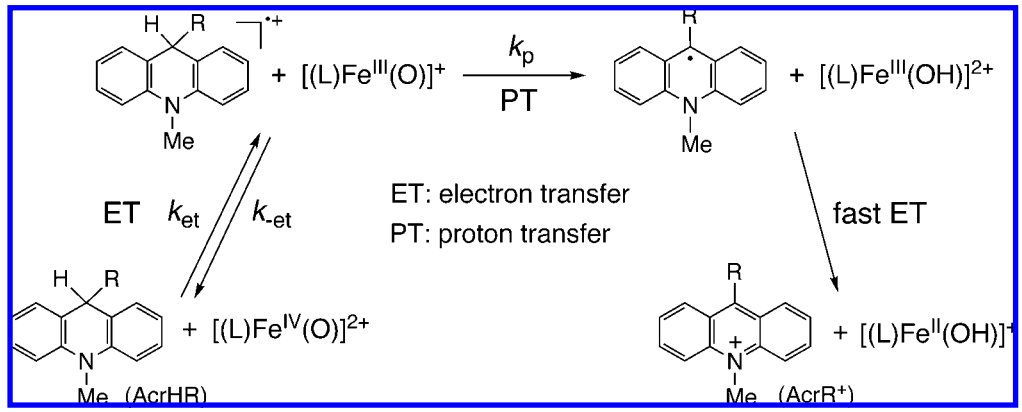

$AcrH_2$ to TolSQ results from the protonation of TolSQ (TolSQ + $H^+ \rightarrow$ $TolSQH^+$), which is confirmed by UV−vis spectral changes of TolSQ in the presence of various amounts of $HClO_4$.[32] Addition of $AcrH_2$ to a deaerated MeCN solution of TolSQ containing $HClO_4$ resulted in the instant appearance of a transient absorption band at $\lambda_{max} = 640$ nm, which is ascribed to the formation of $AcrH_2^{\bullet+}$ that was fully characterized spectroscopically, including ESR.[25] Thus, the occurrence of electron transfer from $AcrH_2$ to $TolSQH^+$ was confirmed by the formation of $AcrH_2^{\bullet+}$ detected by ESR and absorption spectra.[32]

In the present case, addition of AcrDPh to a deaerated MeCN solution of $[(N4Py)Fe^{IV}(O)]^{2+}$ containing $HClO_4$ also results in instant appearance of a transient absorption band at $\lambda_{max} =$ 680 nm, which is ascribed to the formation of $AcrDPh^{\bullet+}$, as shown in Figure 5a.[25] The disappearance of the absorbance at $\lambda_{max} = 680$ nm coincides with the appearance of absorbance at 380 nm due to $[(N4Py)Fe^{II}]^{2+}$ and at 360 nm due to Acr^+−Ph (see Figure 5a, inset). Similarly, formation of $AcrHEt^{\bullet+}$ was observed in the acid-promoted hydride transfer from AcrHEt to $[(N4Py)Fe^{IV}(O)]^{2+}$, as shown in Figure 5b, where the disappearance of the absorbance at $\lambda_{max} =$ 685 nm due to $AcrHEt^{\bullet+}$ coincides with the appearance of absorbance at 360 nm due to Acr^+−Et (see Figure 5b, inset).

The formation of $AcrDPh^{\bullet+}$ in the acid-promoted hydride transfer from AcrDPh to $[(N4Py)Fe^{IV}(O)]^{2+}$ was also confirmed by ESR detection, as shown in Figure 6, where the observed ESR spectrum agrees with the computer-simulated spectrum obtained by using the reported hyperfine coupling constants of $AcrHPh^{\bullet+}$, except for that of deuterium ($I = 1$; a_D(C-9) = 3.4 G), which is reduced by the magnetogyric ratio of proton to deuteron (0.153) and the maximum slope line width ($\Delta H_{msl} =$ 6.0 G).[25] The g-value of the observed spectrum ($g = 2.003$) also agrees with the reported value for $AcrHPh^{\bullet+}$.[25]

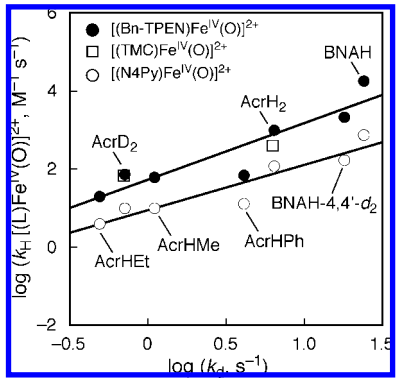

Figure 4. Plot of log k_H for the reactions of $AcrH_2$ with $[(Bn\text{-}TPEN)Fe^{IV}(O)]^{2+}$ (●), $[(TMC)Fe^{IV}(O)]^{2+}$ (□), and $[(N4Py)Fe^{IV}(O)]^{2+}$ (○) vs log k_d for deprotonation of $AcrHR^{\bullet+}$ in MeCN at 298 K.

The electron-transfer rate was determined by the appearance of absorbance at $\lambda_{max} =$ 670 nm due to $AcrHEt^{\bullet+}$ using a stopped-flow technique. The results are shown in Figure 7a, where the appearance of absorbance at $\lambda_{max} = 670$ nm due to $AcrHEt^{\bullet+}$ is followed by the decay, which coincides with the appearance of absorbance at 380 nm due to $[(N4Py)Fe^{II}(OH)]^+$. This is shown as the recovery of bleaching because the transient absorption spectra were measured as the difference spectra from the final spectrum. These results indicate that an acid-promoted electron transfer from AcrHR to $[(N4Py)Fe^{IV}(O)]^{2+}$ occurs first to produce $AcrHR^{\bullet+}$ and $[(N4Py)Fe^{III}(O)]^+$, followed by the generation of $AcrR^{\bullet}$ resulting from the deprotonation of $AcrHR^{\bullet+}$. Subsequently, electron transfer from $AcrR^{\bullet}$ to $[(N4Py)Fe^{III}(OH)]^{2+}$ affords the final products, $AcrR^+$ and $[(N4Py)Fe^{II}(OH)]^+$, as shown in Scheme 2.

The rate of the $AcrHEt^{\bullet+}$ formation obeys first-order kinetics, and the first-order rate constant increases linearly with increasing concentration of $HClO_4$ without exhibiting a saturation behavior (Figure 7b). This indicates that electron transfer from AcrHEt to $[(N4Py)Fe^{IV}(O)]^{2+}$ is promoted by protonation of the one-electron-reduced species ($[(N4Py)Fe^{III}(O)]^+$), which produces $[(N4Py)Fe^{III}(OH)]^{2+}$. It was confirmed that no protonation of $[(N4Py)Fe^{IV}(O)]^{2+}$ was observed in the presence of $HClO_4$.[41] In contrast to the initial electron-transfer step, the rate constant for the decay of $AcrHEt^{\bullet+}$ remains constant with the increase of the $HClO_4$ concentration. This result indicates that the deprotonation of $AcrHEt^{\bullet+}$ is not affected by the presence of $HClO_4$.

In conclusion, we have examined hydride-transfer reactions with a series of NADH analogues and non-heme oxoiron(IV) complexes. The reactivity of non-heme oxoiron(IV) complexes is similar to that of Cl_4Q in hydride-transfer reactions, and there is a linear correlation between the reactivities of non-heme oxoiron(IV) complexes and Cl_4Q. The variation of the reactivity of AcrHR depending on the type of the R group is well correlated with the difference in the deprotonation reactivity of

(39) Anne, A.; Fraoua, S.; Hapiot, P.; Moiroux, J.; Savéant, J.-M. *J. Am. Chem. Soc.* **1995**, *117*, 7412–7421.
(40) Anne, A.; Fraoua, S.; Grass, V.; Moiroux, J.; Savéant, J.-M. *J. Am. Chem. Soc.* **1998**, *120*, 2951–2958.
(41) Virtually no protonation of $[(N4Py)Fe^{IV}(O)]^{2+}$ (1.0×10^{-5} M) occurs in the presence of $HClO_4$ (1.0×10^{-3} M) containing 30% water in MeCN, which is confirmed by the UV−vis spectral titration.

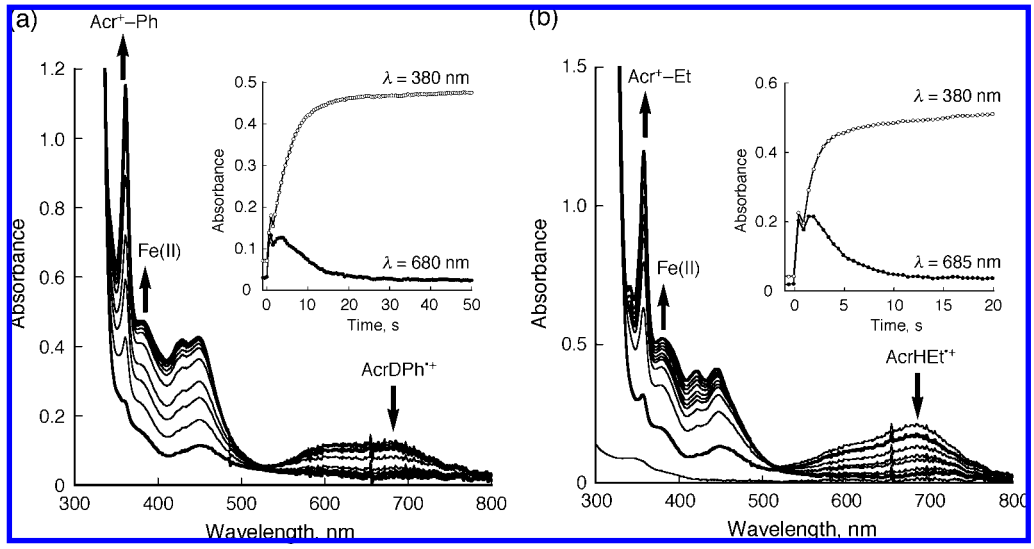

Figure 5. Absorption spectral changes observed upon addition of (a) AcrDPh (2.5×10^{-3} M) and (b) AcrHEt (2.5×10^{-3} M) to a solution of $[(N4Py)Fe^{IV}(O)]^{2+}$ (5.0×10^{-5} M) in MeCN in the presence of $HClO_4$ (2.2×10^{-3} M) at 298 K. Inset: Time profiles of the absorption change at (a) $\lambda =$ 380 and 680 nm and (b) $\lambda = 380$ and 685 nm.

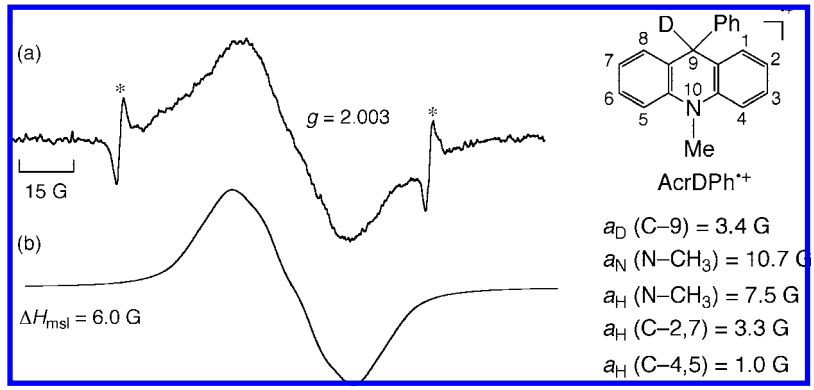

Figure 6. (a) ESR spectrum of $AcrDPh^{\bullet+}$ in frozen MeCN at 77 K after the addition of AcrDPh (1.0×10^{-2} M) to a deaerated solution of $[(N4Py)Fe^{IV}(O)]^{2+}$ (1.0×10^{-4} M) in the presence of $HClO_4$ (1.0×10^{-3} M). Asterisk denotes an Mn^{2+} marker. (b) Computer-simulated spectrum obtained using the hyperfine coupling constants shown above $\Delta H_{msl} = 6.0$ G.

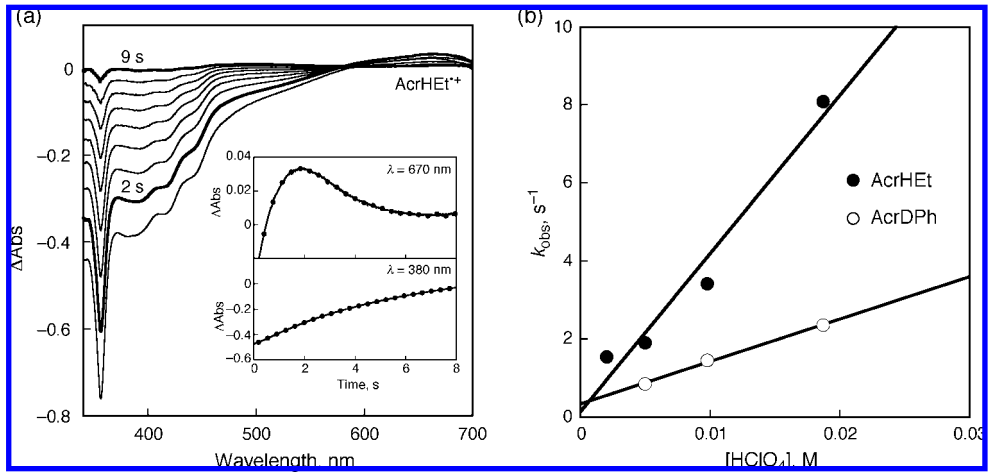

Figure 7. (a) Absorption spectral changes observed upon addition of AcrHEt (1.3×10^{-3} M) to a deaerated solution of $[(N4Py)Fe^{IV}(O)]^{2+}$ (2.5×10^{-5} M) in MeCN in the presence of $HClO_4$ (2.1×10^{-3} M) at 298 K. Inset: Time profiles of the absorption change at $\lambda = 380$ and 670 nm. (b) Dependence of k_{obs} on $[HClO_4]$ in acid-promoted electron transfer from AcrHEt (●) and AcrDPh (○) to $[(N4Py)Fe^{IV}(O)]^{2+}$.

$AcrHR^{\bullet+}$, produced by electron transfer from AcrHR to the hydride acceptors. Thus, hydride transfer from NADH analogues to non-heme oxoiron(IV) complexes may occur via electron transfer from NADH analogues to the oxoiron(IV) complexes,

Scheme 2. Electron-Transfer Pathway in Acid-Promoted Hydride Transfer from AcrHR to $[(L)Fe^{IV}(O)]^{2+}$

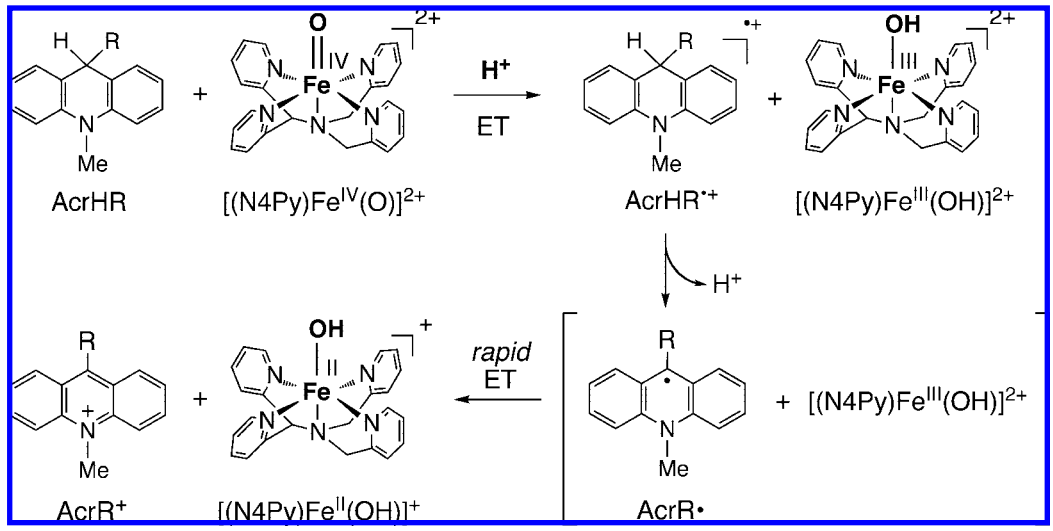

followed by the rate-limiting proton transfer from the radical cations of NADH analogues. Rapid electron transfer from the deprotonated radicals to the Fe(III) complexes then occurs to yield the final products, such as the corresponding NAD^+ analogues and the Fe(II) complexes. The occurrence of electron transfer has been confirmed by the detection of $AcrHR^{\bullet+}$ in the acid-promoted hydride-transfer reactions from AcrDPh and AcrHEt to $[(N4Py)Fe^{IV}(O)]^{2+}$. The present results provide important clues to understand the mechanism(s) of hydride-transfer reactions mediated by high-valent metal−oxo species.[19,42]

Acknowledgment. This work was supported by a Grant-in-Aid (No. 19205019 to S.F.) and a Global COE program, "the Global Education and Research Center for Bio-Environmental Chemistry", from the Ministry of Education, Culture, Sports, Science and Technology, Japan (to S.F.), and the Korea Science and Engineering Foundation through the CRI Program (to W.N.).

JA804969K

(42) Matsuo, T.; Mayer, J. M. *Inorg. Chem.* **2005**, *44*, 2150–2158.